

Steffen Hein

Large eddy approximation of turbulent flow in DSC schemes

Abstract. Large eddy simulation of turbulent flow is given a natural setting in the DSC framework of computational fluid dynamics. Periodic cellular coarse-graining prevents the nodal flow from piling up and preserves its large patterns. The coarsening operations are consistent with the near-field interaction principle of DSC and - therefore - uncomplicated at boundaries. Numerical examples validate the approach.

MSC-classes: 65C20, 65M06, 76D05

Keywords: Navier-Stokes equations, turbulence models, large eddy simulation, DSC schemes

Bad Aibling in spring 2006

1. Introduction

Discrete schemes have to cope with the cursed situation which they create in breaking space into pieces. Mesh cell systems, however fine, can never be perfect substitute for continuous space. Already in linear algorithms they produce artefacts, such as unphysical *spurious* solutions, and more harmful things happen in the non-linear case.

In fluid dynamics, when the non-linear spectral transfer properties of the Navier-Stokes equations (the *energy cascade*; cf. POPE [Po]) come into play beyond the transition to turbulence, eddies are locally excited, down to very short scale; cf. KOLMOGOROV [Ko]. Eddies smaller than the cell size cannot be properly resolved by a mesh of realistic coarseness and thus tend to induce local fluctuations that artificially pile up. Large eddy simulation (LES) aims to discard such divergences through regularizing the flow by means of a suitable averaging filter, and to screen its essential *large patterns* in this way.

LES stands for the most promising line in modern turbulence modelling. The name has been coined by DEARDORFF in 1970, who first applied LES methods to turbulent channel flow [De]. Important elements had yet been kept ready, formerly. Already REYNOLDS [Re] used temporal flow averages that as *Reynolds averages* play still a rôle in conventional turbulence models. In 1922, RICHARDSON [Ri] proposed mesh cell averages for smoothing down local fluctuations. Such so called *box filters* stand today for one line of LES.

Spatial filters of varied type indeed classify modern LES methods. Excellent insight into the state of the art is gained from the recent book of BERSELLI et al. [BIL], which not only exposes the elaborate mathematical framework but also addresses many items of conventional turbulence modelling (the prominent $k-\epsilon$ model of LAUNDER and SPALDING [LS], e.g.).

The present paper differs from many related work in the field in that it sharply separates the natural and technical aspects of turbulent instability and that it strictly focusses on the latter within the *computational context* in hand. The natural part, viz. essentially (modulo discretization) the Navier-Stokes equations for viscous incompressible flow, are thereby treated as a *physical given*. This is in obvious contrast to widespread use. In many conventional turbulence models, as in some lines of LES, turbulent pile-up is controlled by modifying the underlying dynamic equations or even the physical constants. Such models use, for instance, Reynolds number dependent global parameters - usually an *eddy viscosity*, e.g. - or time and space filtered Navier-Stokes equations or any (e.g. stochastic) variant. All this is allowed, of course, as long as it provides numerical data in harmony with observation. Also, a profound change of the inner dynamics can very efficiently delimit turbulence and thus lead to a convergent scheme. It is yet, obviously, tuning the underlying physical phenomenon rather than eliminating the technical cause of divergences that are manifestly an artefact of discretization. (Turbulence is still enigmatic in many respects, yet *divergence* is certainly not a feature of turbulent flow - observed in the continuum of nature, e.g.)

The central point of attack in discarding turbulent pile-up will hence be, in this paper, the weaknesses of discretization, while the Navier-Stokes equations are directly discretized as taken from physics - which not only combats the desaster at the origin, but also yields validated results.

2. DSC schemes

A mesh cell system is not just poor surrogate continuous space, but it has its own structure. Cellular meshes - with that we are dealing here - artificially impose local *cell-boundary duality* upon space [He1]. It is this simple fact that dual scattering channel (DSC) schemes match in a canonical fashion.

DSC schemes are finite volume methods with a singular structure that has repeatedly been treated in technical detail [He1-3]. So, it is sufficient here to recapitulate their essential features in a crash course like manner, following largely [He3]. Every DSC algorithm is characterized by a two-step cycle of iteration which alternately updates vectors within cells and on their interfaces. The updating instructions are explicit and satisfy a near-field interaction principle, which gives rise to a typical scattering process interpretation. A pair of vectors that represent a field on the surface and in the interior of a mesh cell thereby constitutes a *scattering channel*.

The well known primal DSC scheme is JOHNS' TLM algorithm, wherein the scattering channels are visualised by transmission lines. A prototype

algorithm that models viscous Boussinesq incompressible flow has recently been presented [He3].

In the *physical interpretation*, cf. [He1], each scattering channel represents two distributional values $z^p = (p, Z)$ and $z^n = (p^\sim, Z)$ of a physical field Z evaluated, respectively, on the surface and in the interior of a mesh cell. The scalar or vector valued distribution p pertinent to any cell face is called a *port* and p^\sim its *nodal image*, and the two are related by pull-back, viz.

$$(1) \quad (p^\sim, Z) = (p \circ \sigma, Z) = (p, Z \circ \sigma^{-1}),$$

for every Z (of class C^∞ , e.g.), where σ denotes the spatial translation $\sigma : \mathbb{R}^3 \rightarrow \mathbb{R}^3$ that shifts the geometric *node* (i.e. the cell centre) onto the (centre of) the respective face.

It follows that there exists a *scattering channel representation* of DSC states: If M is the mesh cell system and $\partial\zeta$ denotes the boundary of cell $\zeta \in M$ ($\partial\zeta$ is naturally identified with the set of all ports with nodal image in ζ - i.e. with all scattering channels in the cell), then each state permits a unique representation in the space

$$(2) \quad P := \prod_{\zeta \in M} \prod_{p \in \partial\zeta} (z_\zeta^p, z_\zeta^{p^\sim}),$$

with canonical projections $\pi_\zeta^{p, n} : P \rightarrow P_\zeta^{p, n}$ into the port and node components of cell ζ . Furthermore, there is a natural involuntary isomorphism $nb : P \rightarrow P$,

$$(3) \quad nb : (z^p, z^{p^\sim}) \mapsto (z^{p^\sim}, z^p),$$

called the *node-boundary map*, which hence maps P^p onto P^n and vice versa. (The cell index ζ is omitted here and in the following without danger of confusion.)

Of course, nodal images of different ports (e.g. on different faces of the same cell) may represent the same physical field in a node, i.e. coincide as distributions - just as two ports pertinent to neighbouring cells represent the same field on a common face, if they connect two channels on it. In fact, the scattering channel representation of DSC states in (2) is in general highly *redundant* - which can be utilized for process parallelization [He1].

Within the algorithm, the port and node components are updated at even and odd integer multiples, respectively, of half a timestep τ and are usually constantly continued as step functions over the subsequent time intervals of length τ .

Note that *existence*, not necessarily explicit *construction* or *application*, of a scattering channel representation characterizes DSC schemes. Less redundant representations of states are indeed used in real implementations. The scattering channel representation is hence basically a theoretical means for describing (and deriving) certain DSC properties - e.g. the following.

A fundamental principle, closely related to the COURANT-LEVI stability criterion, is *near-field interaction*. It requires that every updated state of

a node or face depends only states (along with their history) in scattering channels connected to the respective node or face - the latter *here* being identified with its adjacent face, if that exists in any neighbouring cell.

As a consequence of near-field interaction, every DSC process allows for an interpretation as a *multiple scattering process* in the following sense.

Let for any process $z = (z^p, z^n)(t)$ *incident* and *outgoing fields* z_{in}^p and z_{out}^n be recursively defined as processes in P^p and P^n , respectively, by setting $z_{in}^p(t) := z_{out}^n(t - \frac{\tau}{2}) := 0$, for $t < 0$, and for $0 \leq t = m\tau; m \in \mathbb{N}$:

$$(4) \quad \begin{aligned} z_{in}^p(t) &:= z^p(t) - nb \circ z_{out}^n(t - \frac{\tau}{2}), \\ z_{out}^n(t + \frac{\tau}{2}) &:= z^n(t + \frac{\tau}{2}) - nb \circ z_{in}^p(t). \end{aligned}$$

Then, at every instant holds $z^p(t) = nb \circ z_{out}^n(t - \frac{\tau}{2}) + z_{in}^p(t)$ and $z^n(t + \frac{\tau}{2}) = nb \circ z_{in}^p(t) + z_{out}^n(t + \frac{\tau}{2})$. Also, near-field interaction implies that every state is only a function of states incident (up to present time t) on scattering channels connected to the respective node or face.

More precisely, by induction holds:

Theorem. There exists a pair of functions \mathcal{R} and \mathcal{C} , defined on back in time running sequences of incident and outgoing fields, respectively, such that for every cell $\zeta \in M$ the process $z_\zeta^n = \pi_\zeta^n \circ z$ complies with

$$(5) \quad z_\zeta^n(t + \frac{\tau}{2}) = \mathcal{R}((z_{in}^p(t - \mu\tau))_{p \in \partial\zeta; \mu \in \mathbb{N}})$$

and the port process $z_\zeta^p = \pi_\zeta^p \circ z$ satisfies

$$(6) \quad z_\zeta^p(t + \tau) = \mathcal{C}((z_{out}^n(t + \frac{\tau}{2} - \mu\tau))_{n \in \partial\zeta; \mu \in \mathbb{N}}). \\ (\text{', |', short-hand for 'in any of the (1 or 2) cells adjacent to' })$$

Remarks

(i) The statements immediately imply that $z_{\zeta, out}^n$ and $z_{\zeta, in}^p$ are themselves functions of states incident on connected scattering channels, since

$$\begin{aligned} z_{\zeta, out}^n(t + \frac{\tau}{2}) &= \mathcal{R}((z_{in}^p(t - \mu\tau))_{p \in \partial\zeta; \mu \in \mathbb{N}}) - z_{\zeta, in}^p(t) \quad \text{and} \\ z_{\zeta, in}^p(t) &= \mathcal{C}((z_{out}^n(t - \frac{\tau}{2} - \mu\tau))_{n \in \partial\zeta; \mu \in \mathbb{N}}) - z_{\zeta, out}^n(t - \frac{\tau}{2}) \end{aligned}$$

(ii) \mathcal{R} and \mathcal{C} are called, respectively, the *reflection* and *connection* maps of the DSC algorithm, and a *field excitation* may be implicit in \mathcal{C} , cf. [He1].

(iii) Near field interaction implies computational stability, if the reflection and connection maps are α -*passive*, i.e. contractive in this sense [He2].

3. Coarse-graining

Mesh cell systems import artificial defects into space, which yet sometimes carry their remedy in themselves - at least in part. For instance, by separating the virtually unresolved cell interior from the coarse-grained skeleton grid, every mesh cell system fixes (and necessarily delimits) the scale of local resolution. A clever design takes into account the coarsening effect of the cellular mesh - which, on the other hand, provides quasi free of charge a basis for large eddy approximation in the DSC setup of computational fluid dynamics. In fact, DSC schemes go along with the 'canonical' large pattern approximation that (in a sense being precised) associates to each quantity its cell average.

The following definition is independent of any particular application and therefore given without reference to fluid dynamics.

Definition (coarse-graining)

For any port $p \in \partial\zeta$ with nodal image p^\sim let B^p denote the set of all ports on $\partial\zeta$, the nodal images of which coincide with p^\sim as distributions. Also, let $w_r \in [0, 1]$; $r \in B^p$, be a set of *weights* such that $\sum_{r \in B^p} w_r = 1$.

Then, every DSC field which in the scattering channel representation on each component $q \in B^p \subset \partial\zeta$ equals (z^q, z^{q^\sim}) with

$$(7) \quad z^{q^\sim} = \sum_{r \in B^p} w_r z^r$$

is named a (*in* ζ *and with weights* w_r) *coarse-grained field* (*pertinent to* p - or also *to its nodal image* p^\sim).

The nodal state of such a field, coarse-grained in any cell, is hence a convex superposition - i.e. a *weighted mean* - of states which represent the field on the cell surface. Also, certainly not too misleading, every substitution of a DSC field with a coarse-grained field that leaves the cell boundary states unchanged is called *coarsening this field* (in any component).

Can such an innocent looking procedure *resolve the turbulence problem*? Remember that our modest aim is repairing some defects of discretization rather than solving the fundamental questions of turbulence - in the way mathematical physics should do that. What matters here is that in the DSC setup of CFD, cf. sect. 4, well-timed periodic coarse-graining of the fluid velocity field efficiently prevents turbulent pile-up and retains the large eddies. The coarsening period should be taken as small as necessary to ensure stability and large enough against the time step (at least five times the latter, by a rule of thumb). Clearly, coarsening inevitably also interferes with the dynamics of the flow. However - since the *skeleton field* on the cell boundaries is left unchanged - the perturbation is minimal and usually negligible. Through removing only the turbulent fluctuations of very short range (below a scale given by cell size) which tend to artificially pile-up, coarsening regularizes the flow only to such a mild degree that its essential *large* patterns are preserved.

4. Fluid dynamics

The port and node distributions of a DSC algorithm can be *finite integrals* - as is the case for the TLM method, where finite path integrals over electric and magnetic fields are evaluated in a discrete approximation to Maxwell's integral equations [He4-6]. In the case in hand, they are simply *Dirac measures* that pointwise evaluate the fields within the cells and on their surfaces, and composites of Dirac measures which approximate the gradients of these fields, cf. [He3], sect.3.

In the *Oberbeck-Boussinesq* approximation [Obb],[Bss] all material fluid properties are assumed as constant - *except fluid density which only in the gravitational term varies linearly with temperature*. The energy equation of a *Boussinesq-incompressible* fluid of velocity \mathbf{u} with thermal diffusivity α , heat source(s) q , and negligible viscous dissipation is then the *convection-diffusion* equation for the temperature T , cf. [GDN],

$$(8) \quad \frac{\partial T}{\partial t} + \mathbf{u} \cdot \operatorname{grad} T = \alpha \Delta T + q.$$

The Navier-Stokes *momentum equations* for a fluid of dynamic viscosity μ , under pressure p , and in a gravitational field of acceleration \mathbf{g} require

$$(9) \quad \frac{\partial}{\partial t} (\varrho \mathbf{u}) + (\mathbf{u} \cdot \operatorname{grad}) (\varrho \mathbf{u}) + \operatorname{grad} p = \mu \Delta \mathbf{u} + \varrho \mathbf{g}.$$

With $\varrho_\infty = \text{const}$ and $\varrho(T) = \varrho_\infty \beta(T(t, \mathbf{x}) - T_\infty)$; $\beta := \varrho^{-1} \partial \varrho / \partial T$, this becomes

$$(10) \quad \frac{\partial \mathbf{u}}{\partial t} + (\mathbf{u} \cdot \operatorname{grad}) \mathbf{u} + \frac{\operatorname{grad} p}{\varrho_\infty} = \frac{\mu}{\varrho_\infty} \Delta \mathbf{u} + \beta(T(t, \mathbf{x}) - T_\infty) \mathbf{g}.$$

Integrating these equations over cell ζ with boundary $\partial\zeta$ and applying Gauss' theorem to integrals over $\Delta = \operatorname{div} \operatorname{grad}$ and over $\mathbf{u} \cdot \operatorname{grad} f + f \operatorname{div} \mathbf{u} = \operatorname{div}(f \mathbf{u})$ yields with time increment τ the following updating instructions for nodal T and \mathbf{u} , the latter and q averaged over the cell volume V_ζ

$$(11) \quad \begin{aligned} T(t + \frac{\tau}{2}) := & T + \tau (T \operatorname{div} \mathbf{u} + q) + \\ & + \frac{\tau}{V_\zeta} \int_{\partial\zeta} (\alpha \operatorname{grad} T - T \mathbf{u}) \cdot dF \end{aligned}$$

and

$$(12) \quad \begin{aligned} \mathbf{u}(t + \frac{\tau}{2}) := & \mathbf{u} + \tau (\mathbf{u} \operatorname{div} \mathbf{u} - \beta(T - T_\infty) \mathbf{g} - \frac{\operatorname{grad} p}{\varrho_\infty}) + \\ & + \frac{\tau}{V_\zeta} \left\{ \int_{\partial\zeta} \frac{\mu}{\varrho_\infty} \operatorname{grad} \mathbf{u} \cdot dF - \int_{\partial\zeta} \mathbf{u} (\mathbf{u} \cdot dF) \right\}. \end{aligned}$$

In equations (11) and (12) the last former updates (at time $t - \tau/2$) of the nodal quantities enter the right-hand sides in the first line, and the former updates (at time t) of the cell face quantities enter the second line. Of course, $\operatorname{div} \mathbf{u}$ vanishes for incompressible flow.

The nodal values of T and \mathbf{u} are updated at the reflection step - after coarsening the velocity field, e.g. with weights proportional to the pertinent cell face areas, whenever the coarsening period is attained - while the port quantities, which enter the surface integrals at the right-hand sides, are updated on the connection step of the iteration cycle. [He3] proceeds with all that - and the special treatment of pressure - in a non-orthogonal hexahedral mesh.

5. Conclusion and Completions

Coarse-graining allows for natural large eddy approximation of turbulent flow in DSC schemes. Since the energy cascade starts long before transition to turbulence - indeed, it is effective over almost the entire energy spectrum [BIL], p.72 ff., a well-timed coarsening routine should escort every DSC fluid flow algorithm, such as proposed in section 4 or [He3]. Periodic coarse-graining significantly improves algorithm stability even in the laminar regime without noticeably perturbing the flow dynamics, if the coarsening period is chosen as outlined in section 3. Precise criteria for a good choice - in relation to mesh refinement, e.g. - should be subject to further study.

Details of the implementation and special applications are clearly beyond the scope of this study. However, it is in order to leave off with some supplementary illustration.

The following graphics are extracted from computations with author's test program **ELFE** (written in C code in the lines of sections 3,4 and [He3]). The results are in keeping with reference computations (FLUENT) and empirical data (RL100-230). The simulations for coaxial line have been carried out with the same operating conditions as in [He3], sect. 6.

References

- [Po] Pope, S.B., *Turbulent flows*, Cambridge University Press, Cambridge 2000.
- [Ri] Richardson, L.F., *Weather Prediction by Numerical Process*, Cambridge University Press, Cambridge 1922.
- [BIL] Berselli, L.C., Iliescu, T., Layton, W.J., *Mathematics of Large Eddy Simulation of Turbulent Flows*, Springer-Verlag, Berlin Heidelberg, 2006
- [LS] Launder, B.E., Spalding, D.B., *Lectures in Mathematical Models of Turbulence*, Academic Press, London 1972
- [MS] Meister, A., Struckmeier, J., *Hyperbolic Partial Differential Equations Theory, Numerics and Applications*, Friedrich Vieweg and Sohn, Göttingen 2002
- [LeVeque] LeVeque, R.J., Mihalas, D., Dorfi, E.A., Müller, E. *Computational Methods for Astrophysical Fluid Flow*, Saas Fee Advanced Courses, 27, Springer-Verlag, Berlin Heidelberg, 1998
- [GDN] Griebel, M., Dornseifer, T., Neunhoeffer, T., *Numerical Simulation in Fluid Dynamics*, SIAM monographs on mathematical modeling and computation, Society for Industrial and Applied Mathematics, 1998
- [ATP] Anderson, D.A., Tannehill, J.C., Pletcher, R.H., *Computational Fluid Mechanics and Heat Transfer*, series in computational methods in mechanics and thermal sciences, Hemisphere Publishing Corporation, 1984
- [Bss] Boussinesq, J., *Théorie Analytique de la Chaleur*, Gauthiers-Villars, 2., Paris 1903

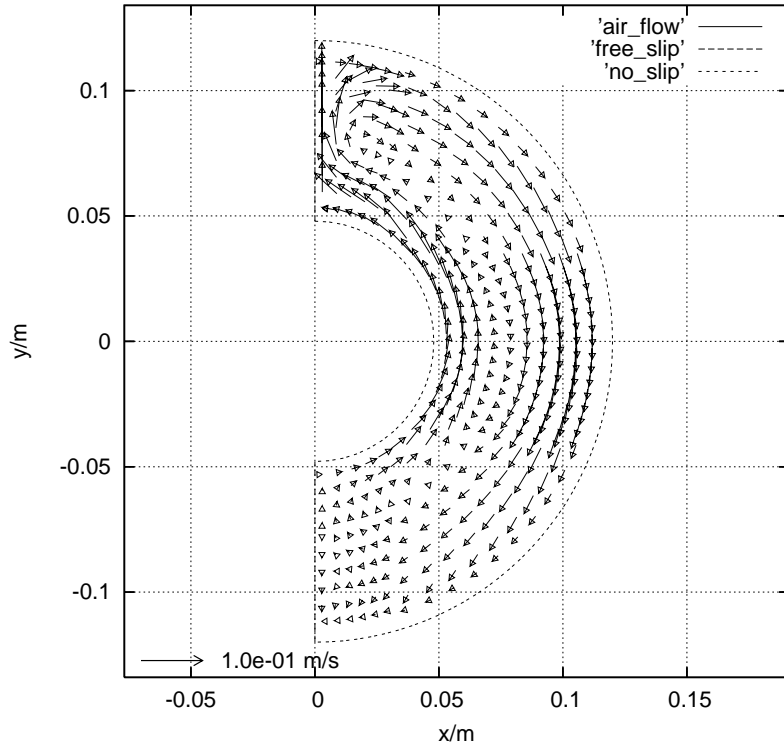


Fig. 1. Air convection in horizontal coaxial line RL100-230 ;
transverse section [reference arrow: 0.1 ms^{-1}].

- [Ko] Kolomogorov, A.N., The local structure of turbulence in incompressible viscous fluids for very large Reynolds number. *Dokl. Akad. Nauk SSR*, vol. 30, pp. 9-13, 1941
- [De] Deardorff, J.W., A numerical study of three-dimensional turbulent channel flow at large Reynolds numbers. *J. Fluid Mech.*, vol. 41, pp. 453-480, 1970
- [Re] Reynolds, O., On the dynamic theory of the incompressible viscous fluids and the determination of the criterion. *Philos. Trans. Roy. Soc. London Ser. A*, vol. 186, pp. 123-164, 1895
- [OBB] Oberbeck, A., Über die Wärmeleitung der Flüssigkeiten bei Berücksichtigung der Strömung infolge Temperaturdifferenzen., *Ann. Phys. Chem.*, vol. 7, pp. 271-292, 1879
- [JoB] Johns, P.B., Beurle R.L., Numerical solution of 2-dimensional scattering problems using transmission line matrix, *Proc. IEEE*, vol. 118, pp. 1203-1208, 1971
- [He1] Hein, S., Dual scattering channel schemes extending the JOHNS Algorithm <http://arxiv.org/abs/math.NA/0309261>, March 2004
- [He2] Hein, S., On the stability of dual scattering channel schemes, <http://arxiv.org/abs/math.NA/0405095>, May 2004
- [He3] Hein, S., A DSC approach to computational fluid dynamics, <http://arxiv.org/abs/math.NA/0510070>, October 2005

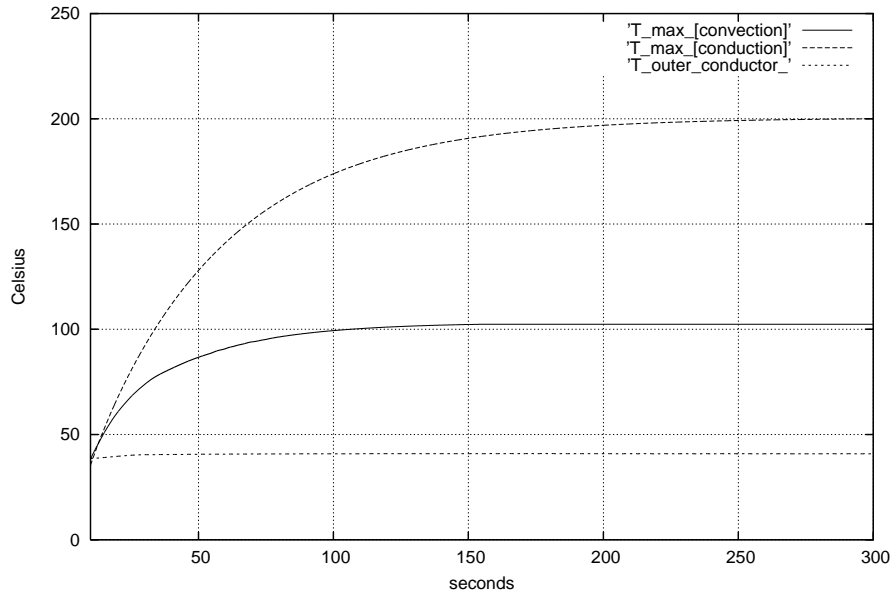


Fig. 2. Heating process in coaxial line RL100-230 ;
 temperature maximum vs. time from power-on,
 convection compared to - fictitious - pure conduction.
 [Transmitted power 160 kW CW, frequency 100 MHz,
 outer conductor cooled at 40 degrees Celsius.]

- [He4] Hein, S., Synthesis of TLM Algorithms in the Popagator Integral Framework, Proceedings of the 2nd. Int. Workshop on Transmission Line Matrix Modeling (TLM) - Theory and Applications, pp. 1-11, München, October 1997 (invited paper)
- [He5] Hein, S., Finite-difference time-domain approximation of Maxwell's equations with nonorthogonal condensed TLM mesh, Int. J. Num. Modelling, vol. 7, pp. 179-188, 1994
- [He6] Hein, S., TLM numerical solution of Bloch's equations for magnetized gyrotropic media, Appl. Math. Modelling, vol. 21, pp. 221-229, 1997

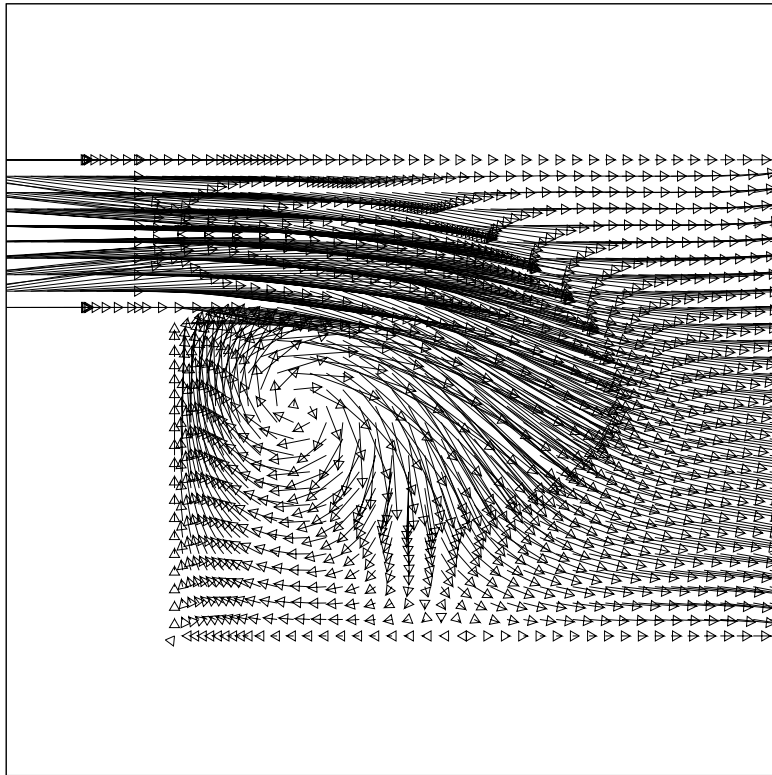


Fig. 3. Jet over backward facing step ;
shock wave and vortex shortly after fluid injection.
[$Re \approx 5 \times 10^6$]

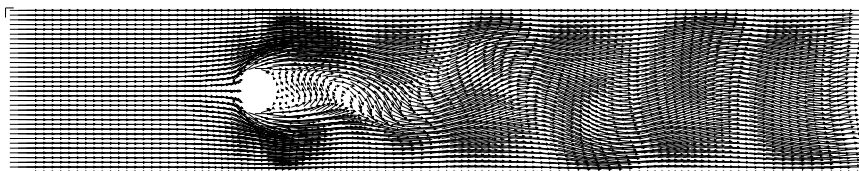


Fig. 4. Kármán vortex street behind cylinder
[snapshot of oscillating flow].